Synthesis, Structure, Magnetic and Antibacterial Properties of polymeric $[M(Quin)_2(N(CN)_2)_2]_\infty$ (M = Mn(II), Co(II); Quin = quinoline)

I Wayan Dasna[1,2]*, Ubed Sonai Fahruddin Arrozi[1], Husni Wahyu Wijaya[1,2], Sutandyo Dwija Laksmana[1], & Stéphane Golhen[3]

[1]Department of Chemistry, State University of Malang (Universitas Negeri Malang), Jl. Semarang 5, Malang, Jawa Timur, Indonesia 65145
[2]Centre of Advanced Material for Renewable Energy, State University of Malang (Universitas Negeri Malang), Jl. Semarang 5 Malang, Jawa Timur, Indonesia 65145
[3]University of Rennes, CNRS, ISCR (Institut des Sciences Chimiques de Rennes) – UMR 6226, 35000 Rennes, France
*Email: idasna@um.ac.id

Abstract. Two complexes of $[Mn(Quin)_2(N(CN)_2)_2]_\infty$ (**1**) and $[Co(Quin)_2(N(CN)_2)_2]_\infty$ (**2**) were synthesized and characterized. The as-synthesized complexes crystallized in a triclinic lattice with a space group of P-1. The unit cell parameter of **1** was a = 7.5207(14) Å, b = 7.7729(16) Å, c = 9.5968(15) Å, α = 96.388(6) º, β = 112.617(5) º, γ = 102.751(6) º, while for complex **2** it was a = 7.3942(10) Å, b = 7.7960(10) Å, c = 9.4907(13) Å, α = 96.631(4) º, β = 112.742(4) º, γ = 102.458(4) º. The magnetic properties and antimicrobial properties of both polymeric complexes were examined by magnetic susceptibility and diffusion techniques, respectively. Complexes **1** and **2** both showed antiferromagnetic properties and had a higher inhibitory effect on the growth of *Staphylococcus aureus* than *Salmonella typhi*.

Keywords: *Manganese(II) complex, Cobalt(II) complex, quinoline ligand, antiferromagnetic; antibacterial.*

1 Introduction

In the last decade, antibiotic resistance of *Salmonella typhi* and *Staphylococcus aureus* bacteria has been detected by biomedical scientists [1,2]. Both are dangerous bacteria, especially in tropical countries, leading to the necessity of finding novel antibacterial compounds [3]. Complex compounds consisting of transition metal and N-heterocyclic ligands with free electron pairs have been reported for antimicrobial candidates [4-6]. There are two main criteria for complexes to have antibacterial properties. Firstly, the central atom must be capable of interacting with the DNA of the bacteria to form a more stable interaction, resulting in bacteria deactivation and regeneration [7,8]. Secondly, the presence of free electron pairs from ligands can polarize lipids on the bacterial surface, forcing the organelles to come out [5,6]. Some of the ligands that have

Received July 15th, 2022, Revised November 25th, 2022, Accepted for publication January 21st, 2023
 ISSN: 2337-5760, DOI: 10.5614/j.math.fund.sci.2022.54.2.4

been studied for their potential as antibacterial compounds are quinoline and dicyanamide derivates [4,5,7-11].

Several $[M(L)_x]$ complexes (M = transition metals, L = quinoline or cyanamide derivate) have been synthesized and reported to function as antibacterial compounds [9,12-14]. Although cyanamide ligands are widely used as starting material of supramolecular compounds [15-18] and can act as monodentate, bidentate, and bridging ligands [19-21], complexes formed by these compounds potentially have antibacterial properties due to their free electron pairs in the nitrogen atom [13,22]. Likewise, quinoline ligands have high electron density and the potential to interact with the bacterial surface. Furthermore, complexes with metal ions of Mn^{2+}, Co^{2+}, Ni^{2+}, and Cu^{2+} with $[N(CN)_2]^-$ ligands have been reported to have antibacterial properties [5,13,14]. They have different bacterial inhibition due to differences in the metal ions, which can affect their ability to polarize bacterial components [23]. Thus, developing complexes with high antibacterial properties by combining the properties of metal ions and ligands is still required.

In this study, complexes of $[M(Quin)_2(N(CN)_2)_2]_\infty$ with M = Mn^{2+} and Co^{2+} were synthesized and characterized. These two metal ions generally form stable complexes in an octahedral geometry and can form chain-like structures due to $[N(CN)_2]^-$ bridging ligands. Further, the quinoline ligands with high electron density will coordinate to the metal ions. The combination of these two metal ions with these two types of ligands is expected to have good interaction with functional groups in the bacterial DNA and mitochondria and reduce bacterial activity. The structure and the magnetic properties of the as-synthesized crystals are also reported in this paper.

2 Experimental Section

2.1 Materials

$Mn(NO_3)_2.4H_2O$ (≥97%), C_9H_7N (≥97%), and $NaN(CN)_2$ (96%) were purchased from Sigma Aldrich. $CoCl_2.6H_2O$ (99%) and CH_3OH (99.9%) without further purification were obtained from Merck.

2.2 Instrumentation

Single crystals of $[Mn(Quin)_2(N(CN)_2)_2]_\infty$ (**1**) and $[Co(Quin)_2(N(CN)_2)_2]_\infty$ (**2**) complexes were measured on an APEX II diffractometer equipped with an Mo Kα radiation source. All structures were solved and refined with SHELXTL and SHELXL programs [G. M. Sheldrick, Acta Crystallogr., Sect. A: Found.

Crystallogr., 2008, 64, 112-122] respectively. A Shimadzu IR Prestige-21 spectrophotometer with KBR pellet was used to record FTIR spectra.

2.3 Synthesis of Complexes

Complex **1**. $Mn(NO_3)_2.4H_2O$ salt (0,2510 g; 1 mmol) was slowly added to 10 mL of methanolic solution of quinoline (0,23 mL; 2 mmol) and stirred for 2 h, resulting in an orange solution. The second ligand, $NaN(CN)_2$ (0,1780 g; 2 mmol), was slowly added to the mother liquor solution and stirred for 4 h. The resulting solution was slowly evaporated to obtain white cubic-shaped crystals after 10 days. Melting point 208 °C, IR (cm^{-1}); 2177 (C≡N); 1148 (C=N).

Complex **2**. $CoCl_2.6H_2O$ salt (0,24 g; 1 mmol) was added to 10 mL of methanolic solution of quinoline (0,23 mL; 2 mmol) and stirred at 70 °C for 2 h, giving a blue solution. The second ligand, $NaN(CN)_2$ (0,1780 g; 2 mmol), was then added to the mother liquor and stirred for 4 h. The complex solution was filtered and slowly evaporated, forming red needle-shaped crystals after 10 days. Melting point 230 °C, IR (in cm^{-1}); 2183 (C≡N); 1147 (C=N).

2.4 Antibacterial Study

The antibacterial activity of both complexes was evaluated using the diffusion technique with *Salmonella typhi* and *Staphylococcus aureus* bacteria. Both bacteria stored in NA were suspended in NaCl solution as nutrient on NB agar media. The bacteria culture was inoculated into the agar media for 500 μL until evenly distributed throughout the test media. Paper disks of 6 mm in diameter were immersed into the test, reactant, and control solutions for 20 minutes. The concentration of the sample and control was set to 1 mg/mL. The samples were incubated for 1 day at 37 °C and the diameter of the inhibition zone was observed. Analysis of antibacterial activity was carried out by measuring the clear area, which indicates the inhibition of microorganism growth by the antibacterial agent. Measurements of the diameter of the inhibition zone of bacterial growth were compared among the complexes, starting materials of the complexes (metal salts, ligands, and solvent), and chloramphenicol as positive control.

3 Results and Discussion

3.1 Synthesis and Structure of Complexes

Complexes **1** and **2** were synthesized using the direct reaction method by mixing both metal salts and quinoline. The addition of $NaN(CN)_2$ was performed after the former step had proceeded for 2 h, allowing the $N(CN)_2$ ligand to slowly insert between metal ions and act as a bridging ligand. Single crystals of both complexes were obtained by slow evaporation with color and shape depending on the metal

ions of the complexes. **1** and **2** are stable complexes at room temperature and undergo decomposition at 230 °C for complex **1** and 208 °C for complex **2** as visually assessed from their change in color.

Table 1 Crystal data and structure refinement for **1** and **2**.

	1	**2**
Empirical formula	C_{22} H_{14} Mn N_8	C_{22} H_{14} Co N_8
Formula weight	445.35	449.34
Temperature	150(2)K	150(2) K
Wavelength	0.71073 Å	0.71073 Å
Crystal system	Triclinic	Triclinic
Space group	P -1	P -1
Unit cell dimensions	a = 7.5207(14) Å b = 7.7729(16) Å c = 9.5968(15) Å α= 96.388(6)° β = 112.617(5)° γ = 102.751(6)°	a = 7.3942(10) Å b = 7.7960(10) Å c = 9.4907(13) Å α = 96.631(4)° β = 112.742(4)° γ = 102.458(4)°
Volume	492.96(16) $Å^3$	480.52(11) $Å^3$
Z	1	1
Density (calculated)	1.500 Mg/m^3	1.553 Mg/m^3
Absorption coefficient	0.698 mm^{-1}	0.922 mm^{-1}
F(000)	227	229
Theta range for data collection	2.753 to 27.113°	3.015 to 27.562°.
Index ranges	$-9 \le h \le 9$, $-9 \le k \le 9$, $-8 \le l \le 12$	$-9 \le h \le 5$, $-9 \le k \le 10$, $-12 \le l \le 12$
Reflections collected	6467	4765
Independent reflections	2135 [R(int) = 0.0354]	2166 [R(int) = 0.0290]
Completeness to theta	θ = 25.242°, 98.9 %	θ = 25.242°, 99.5 %
Refinement method	Full-matrix least-squares on F^2	
Data / restraints / parameters	2135 / 0 / 142	2166 / 0 / 142
Goodness-of-fit on F^2	1.167	1.058
Final R indices [I>2σ(I)]	R1 = 0.0419, wR2 = 0.0992	R1 = 0.0541, wR2 = 0.1393
R indices (all data)	R1 = 0.0466, wR2 = 0.1022	R1 = 0.0589, wR2 = 0.1450
Largest diff. peak and hole	0.565 and -0.470 $e.Å^{-3}$	2.779 and -0.561 $e.Å^{-3}$

Single crystal XRD was carried out to determine the crystal structure of both complexes, as summarized in Table 1. Both complexes had the same structural arrangement, with a metal ion at the center, surrounded by six ligands in a distorted octahedral shape. The metal ions are located on an inversion center, which means that the complex is centrosymmetric, as shown in Figure 1. The metal ions are coordinated to the nitrogen atom of two quinoline ligands in an axial position. The equatorial position is occupied by $[N(CN)_2]^-$ as bridging ligand to form a 1D chain parallel to the *a* axis (Figure 1). This structure was also observed in the previously reported complex of $[Cu(NITpPy)_2(N(CN)_2]_2$ [19].

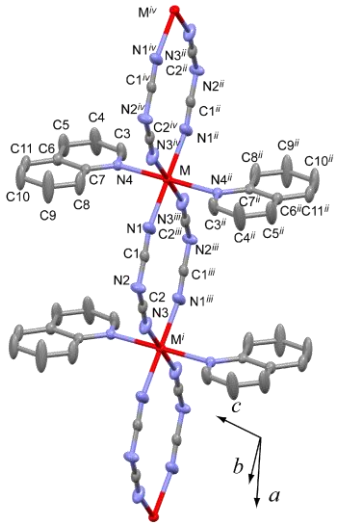

Figure 1 View of polymeric compound $[M(Quin)_2(N(CN)_2)]_\infty$ developed along the *a* axis. (The labeling scheme is the same for both the M = Mn and the Co compound). Symmetry transformations used to generate equivalent atoms: ^{i}x+1,y,z; ^{ii} -x,-y,-z; ^{iii} -x+1,-y,-z; ^{iv} x-1,y,z.

Selected bond lengths and bond angles of the centrosymmetric complexes are tabulated in Table 2. The bond length of the Mn ions and the quinoline ligand is indicated by the distance of Mn – N4 (Figure 1), i.e., 2.3432(18) Å. This length is slightly greater than the bond length between the Mn ions and the $N(CN)_2$ ligand, as shown by the distance of Mn – N (1) = 2.201(2) Å and Mn – N (3) ^{iii} = 2.206(2) Å (Figure. 1). It shows the steric effect of the aromatic ring in the quinoline ligand. A shorter bond length was observed for complex **2**, as shown in Table 2. The distance of Co – N (4) was observed to be 2.225(2) Å, while Co – N (1) and Co – N (3) ^{iii} were 2.109(2) and 2.117(2) Å, respectively.

The higher bond length of Mn – N compared to Co – N is most likely due to the ionic atomic radius of the metal ions as well as the bond strength between the metal ions and N as electron-donating atoms. The bond angles of N1-M-N4 were 93.00(7) and 92.60(8) for complex **1** and **2**, respectively (obviously, the centrosymmetric bond angle of N4-M-N1^{ii} was observed to be 87.00(7) in complex **1** and 87.40(8) in complex **2**. This distorted structure is caused by the steric hindrance of the quinoline and the bridging ligand of $N(CN)_2$. This steric hindrance effect can be observed in the bond angles and distances of the complex.

Table 2 Selected bond lengths [Å] and angles [°] * for **1** and **2**.

	1 (M = Mn)	**2 (M = Co)**		**1 (M = Mn)**	**2 (M = Co)**
M-N(1)	2.201(2)	2.109(2)	N(4)-C(7)-C(6)	122.1(2)	121.9(2)
M-N(3)^{iii}	2.206(2)	2.117(2)	C(8)-C(7)-C(6)	118.6(2)	118.4(2)
M-N(4)	2.3432(18)	2.225(2)	C(9)-C(8)-C(7)	119.6(3)	120.1(2)
C(1)-N(1)	1.148(3)	1.151(4)	C(8)-C(9)-C(1)	121.7(3)	121.0(3)
C(1)-N(2)	1.303(3)	1.305(4)	C(11)-C(10)-C(9)	119.7(3)	120.5(3)
C(2)-N(3)	1.152(3)	1.153(4)	C(10)-C(11)-C(6)	120.5(2))	120.2(3)
C(2)-N(2)	1.303(3)	1.302(4)	N(1)-M-N(3)^{iii}	87.71(10)	86.92(9)
C(3)-N(4)	1.312(3)	1.325(4)	N(1)-M-N(3)^{iv}	92.29(10)	93.08(9)
C(3)-C(4)	1.394(4)	1.407(4)	N(1)-M-N(4)^{ii}	87.00(7)	87.40(8)
C(4)-C(5)	1.360(4)	1.361(4)	N(1)-M-N(4)	93.00(7)	92.60(8)
C(5)-C(6)	1.399(4)	1.412(4)	N(1)^{ii}-M-N(4)	87.00(7)	87.40(8)
C(6)-C(7)	1.411(3)	1.419(4)	N(3)^{iii}-M-N(4)	86.68(7)	87.17(8)
C(6)-C(11)	1.408(3)	1.423(4)	C(1)-N(1)-M	159.8(2)	160.4(2)
C(7)-N(4)	1.381(3)	1.377(3)	C(2)-N(2)-C(1)	119.9(2)	118.6(2)
C(7)-C(8)	1.399(3)	1.417(4)	C(2)-N(3)-M^{i}	161.2(2)	161.9(2)
C(8)-C(9)	1.364(4)	1.375(4)	C(3)-N(4)-C(7)	117.1(2)	117.2(2)
C(9)-C(10)	1.402(4)	1.407(4)	C(3)-N(4)-M	113.72(15)	113.76(17)
C(10)-C(11)	1.339(4))	1.352(5)	C(7)-N(4)-M	129.16(14)	129.03(18)
N(1)-C(1)-N(2)	175.4(3)	174.6(3)	N(1)…N(2)…N(3)	124.8(1)	123.8(1)
N(3)-C(2)-N(2)	174.1(3)	174.2(3)			
N(4)-C(3)-C(4)	124.3(2)	124.6(3)			
C(5)-C(4)-C(3)	119.1(3)	118.6(3)			
C(4)-C(5)-C(6)	119.6(2)	119.6(2)			
C(5)-C(6)-C(7)	117.7(2)	118.1(2)			
C(5)-C(6)-C(1)	122.4(2)	122.1(2)			
C(7)-C(6)-C(11)	119.9(2)	119.8(3)			
N(4)-C(7)-C(8)	119.3(2)	119.7(2)			
N(1)…N(3)	4.343(3)	4.327(3)			

*Symmetry transformations used to generate equivalent atoms: ^{ii} -x,-y,-z; ^{iii} -x+1,-y,-z; ^{iv} x-1,y,z.

Figure 1 shows the two complexes forming polymeric crystals, with the $[N(CN)_2]^-$ ligand forming a chain along the axis. The shortest intra-chain interaction was observed between nitrogen atoms of the same $[N(CN)_2]^-$ ion and between two $[N(CN)_2]^-$ ions, i.e., 4.343(3) Å and 5.312(4) Å for complex **1**; 4.327(3) Å and 5.206(5) Å for complex **2**. The distortion of the bond angle in complex **2** was higher than that in complex **1**, since the ionic radius of Co(II) is smaller than that of Mn(II).

In Figures 2 and 3, the 1D structure of complexes **1** and **2** is shown, where the $[N(CN)_2]^-$ ligand acts as a bridging ligand (μ1 and μ3), connecting two metal ions in a bidentate manner. As shown in Figure 3, the quinoline molecules have *trans* conformation with each other in the unit cell between the square corners of the four chains of the complex along the *a*-axis. Such an arrangement can create voids

in the center of the lattice, which can promote the role of these compounds as antibacterial agents or catalysts. A similar structure has been found in complexes consisting of $[N(CN)_2]^-$ and 2-NITpPy ligands with Mn(II) and Co(II) metal ions [24,25]. Both complexes also have the same structure as complexes containing oxoquinoline as a derivate of quinoline with dicyanamide as ligand [26]. The dicyanamide bridge formed is almost the same as observed in the $[M_2(enbzpy)(dca)_4]_n$ (M = Cu(II) Ni(II)), $[Fe(dmbpy)(\mu_{1,5}\text{-}dca)_2]$, $[Mn(dca)_2(dmdpy)]$, and $[Co(dca)_2(dmdpy)]$ complexes [27-29].

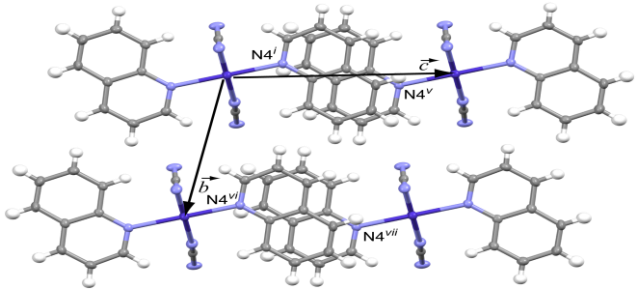

Figure 2 Packing of compound $[M(Quin)_2(N(CN)_2)_2]_\infty$. The labeling scheme is the same for both M = Mn and Co compounds. Symmetry transformations used to generate equivalent atoms: ^{i}x+1,y,z;^{v} 1-x,-y,1-z; ^{vi} x+1, y+1,z; ^{vii} 1-x, 1-y, 1-z.

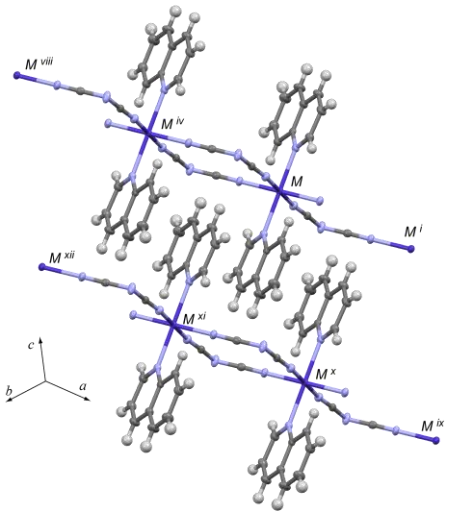

Figure 3 1-D chain structure of $[M(Quin)_2(N(CN)_2)_2]_\infty$ (M = Co(II), Mn(II)) along the a axis with $N(CN)_2$ acting as bridging ligand with symmetries ^{i}: 1+x, y, z; ^{iv}: x-1, y, z; ^{viii}: x-2, y, z; ^{ix}: 1+x, y, z-1;. ^{x}: x, y, z-1;. ^{xi}: x-1, y, z-1;. ^{xii}: x-2, y, z-1.

The 1D chain structure of these complexes could also be detected by FTIR. As depicted in Figure 4, one of the -C≡N functional groups from the $[N(CN)_2]^-$ ligand was observed at 2177 cm^{-1} for complex **1** and 2183 cm^{-1} for complex **2**, shifting towards a higher wavenumber. This indicates that both N atoms of the $[N(CN)_2]^-$ ligand are coordinated to metal ions (Figure 3).

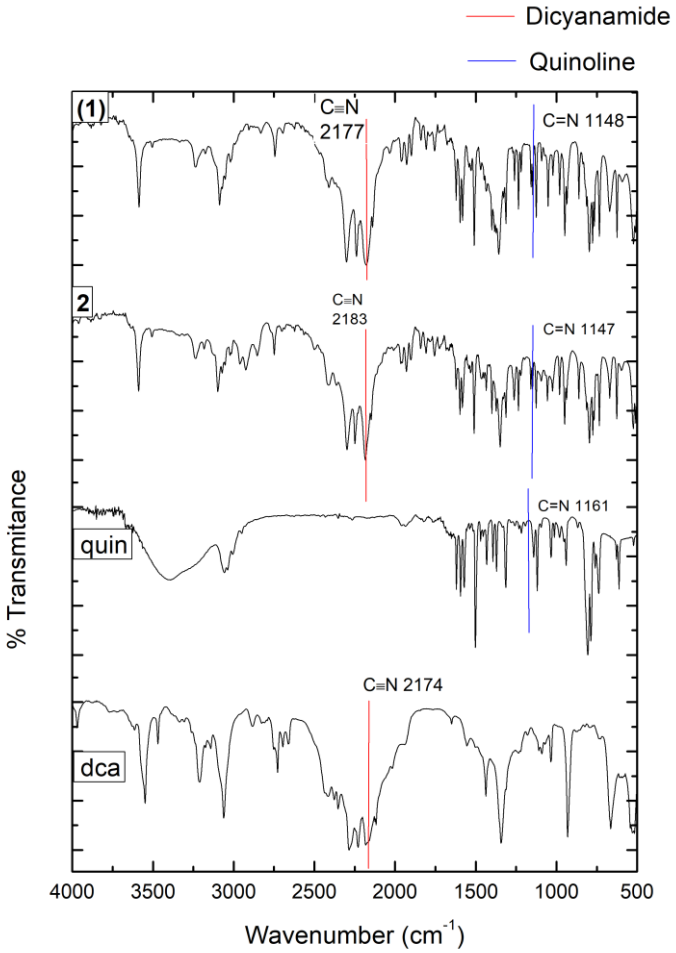

Figure 4 FTIR spectra of **1**, **2**, quinoline, and sodium dicyanamide.

The conductivity of both complexes was measured to understand the ionization in the methanolic solution. As tabulated in Table 3, both complexes showed lower conductivity compared to their precursors, except for quinoline. This indicates that both complexes remained in molecular form in that solvent.

Table 3 Electrical conductivity of complexes and their precursors.

No	Compound	C(mg.mL^{-1})	$\sigma(\mu$S.cm^{-1})
1.	Methanol	-	5.29
2.	Quinoline (MeOH)	1	3.06
3.	$NaN(CN)_2$ (MeOH)	1	120.3
4.	$Mn(NO_3)_2$ (MeOH)	1	500.0
5.	$CoCl_2$ (MeOH)	1	86.0
6.	$Mn(quin)_2(N(CN)_2)_2$ (MeOH)	1	38.0
7.	$Co(quin)_2(N(CN)_2)_2$ (MeOH)	1	32.4

3.2 Magnetic Properties

The temperature dependences of the magnetic susceptibility for complexes **1** and **2** were measured in the temperature range from 2K to 300K using an applied field of 1,000 Oe. At room temperature, the value of $\chi_M T$ for complex **1** was 4.2 cm^3.K.mol^{-1}, which is equal to S = 5/2 spins of Mn^{II} (Figure. 5a). This value decreased when the temperature was lowered, which indicates antiferromagnetic interactions. The χ_M T value for complex **2** at room temperature was close to 3.1 cm^3.K.mol^{-1}, which is higher than the spin-only of cobalt(II) in the absence of exchange coupling (Figure 5b). The magnitude of the magnetic susceptibility can be attributed to a significant orbital contribution from the octahedral Co(II) ions. The decrease of χ_M T at lower temperature indicates weak antiferromagnetic interactions. Both complexes show no interaction between metal ions since the $[N(CN)_2]^-$ ligand has sufficient length to prevent interaction between adjacent metal ions.

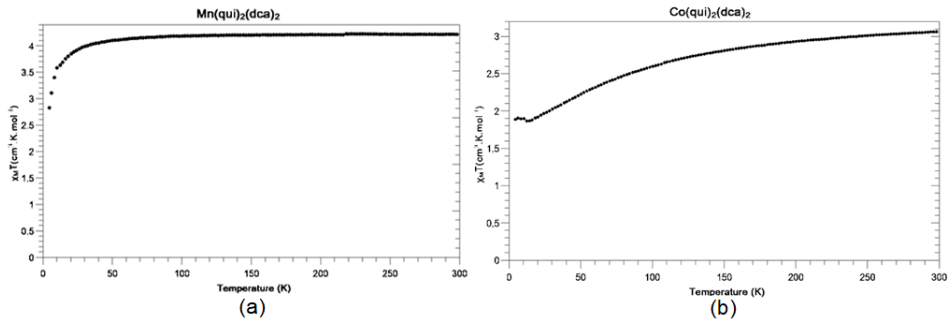

Figure 5 Experimental χ_M T vs temperature for complex **1** (a) and complex **2** (b).

3.3 Antibacterial Activities

The diffusion method with Millner-Tunner agar media was used to evaluate the antibacterial properties of the complexes. The antibacterial activity is presented in Table 4. As presented in Table 4, complexes **1** and **2** showed similar spot

diameters. This could be because the atomic radii of the metal ions were not too large and the effect of the ligands on both complexes was the same [23]. Moreover, both complexes showed similar antibacterial activity, where the zone of inhibition was larger for *Staphylococcus aureus* than for *Salmonella typhi* (Table 4, Entry 1 & 2). A similar trend has also been observed in another complex containing dicyanamide ligand, i.e., $[Mn(2\text{-ampy})_2(\mu\text{-}_{1,5}\text{-dca})_2]_n$ (2-ampy = 2-Aminopyridine) [26]. Moreover, as displayed in Table 4 (Entry 1-2 and 6-10), samples **1** and **2** showed a slightly better inhibitory effect on both bacteria compared to their starting materials (metal salts, free ligands, and methanol). Yet, they showed inferiority in compassion to chloramphenicol (+).

Complexes **1** and **2** both showed a higher inhibitory effect on *Salmonella typhi* compared to $[Mn(2\text{-ampy})_2(\mu\text{-}_{1,5}\text{-dca})_2]n$, although both had a lower inhibitory effect on *Staphylococcus aureus* compared to the latter. As expected, an isostructural complex with pyrazinamide ligand (PZA), $\{[Mn(\mu_{1,5}\text{-dca})_2(PZA)_2](PZA)_2\}_n$, shows a greater inhibitory effect compared to samples **1** and **2**, since PZA contains more atoms with free electron pairs (Entry 3, Table 4). The more polar the side groups, the stronger the ability to polarize the bacteria [14,30].

Table 4 Antibacterial test.

Entry	Sample	Zone of inhibition (mm)		Remarks
		Salmonella typhi	***Staphylococcus aureus***	
11	Chloramphenicol (+)	24.9	8.8	This work
3	$\{[Mn(\mu1,5\text{-dca})_2(PZA)_2](PZA)_2\}_n$	24.5	13.6	[14]
4	$[Mn(2\text{-ampy})_2(\mu1,5\text{-dca})_2]_n$	1.25	12.5	[29]
5	$Co(2\text{-ampy})_2(dca)_2$	8.5	6.0	[5]
8	$CoCl_2.6H_2O$	6.05	6.6	This work
10	Methanol	6.55	6.4	This work
1	**1**	5.9	6.7	This work
2	**2**	5.8	6.85	This work
7	$Mn(NO_3)_2.4H_2O$	5	6.65	This work
9	$NaN(CN)_2$	5	6.5	This work
6	Quinoline	5	6.2	This work

4 Conclusion

Complexes of $[M(Quin)_2(N(CN)_2)_2]_\infty$ (M = Mn(II), Co(II)) were successfully synthesized using the direct method. Both are 1D polymeric crystals with an octahedral geometry along the metal ions with the $[N(CN)_2]^-$ ligand acting as

bridging ligand bidentate μ1 and μ3. Both complexes had similar magnetic properties, i.e., antiferromagnetic at room temperature. Their antibacterial activity toward *S. Typhi* and *S. aureus* was higher than that of the precursors.

5 Supplementary Material

Crystallographic data for structural analysis were deposited with Cambridge Crystallographic Data Centre, CCDC no. 2184062 for $[Mn(Quin)_2(N(CN)_2)_2]_\infty$ and CCDC no. 2184061 for $[Co(Quin)_2(N(CN)_2)_2]_\infty$. Copies of this information may be obtained from the CCDC and FIZ Karlsruhe Deposition Teams, e-mail: deposit@ccdc.cam.ac.uk or from the Cambridge Crystallographic Data Centre: https://www.ccdc.cam.ac.uk.

Acknowledgement

The authors acknowledge Universitas Negeri Malang for its support of this research with project no. 5.3.493/UN/32.14.1/LT/2021. Single crystal data collection was carried out at the Centre de Diffractométrie X from the Institut des Sciences Chimiques de Rennes (UMR 6226 Université de Rennes – CNRS). SG thanks Thierry Roisnel for data collection.

References

[1] Fair, R. J. & Tor, Y., Antibiotics and Bacterial Resistance in the 21st Century, *Perspect. Medicin. Chem.*, (6), pp. 25–64, 2014.

[2] Adzitey, F., *Antibiotic Classes and Antibiotic Susceptibility of Bacterial Isolates from Selected Poultry; A Mini Review*, World Vet J., **5**(53), pp. 36–41, 2015.

[3] Hemeg, H. A., *Nanomaterials for Alternative Antibacterial Therapy*, Int. J. Nanomedicine, **12**, pp. 8211–8225, 2017.

[4] Witwit, I. N., Motaweq, Z. Y. & Mubark, H. M., *Synthesis, Characterization, and Biological Efficacy On New Mixed Ligand Complexes Based from Azo Dye of 8-Hydroxy Quinoline as A Primary Ligand and Imidazole as A Secondary Ligand with Some of Transition Metal Ions*, J. Pharm. Sci. Res., **10**(12), pp. 3074–3083, 2018.

[5] Colette, A., Yuoh, B., Agwara, M.O., Yufanyi, D. M., Conde, M. A., Jagan, R. & Eyong, K. O., *Synthesis, Crystal Structure, and Antimicrobial Properties of a Novel 1-D Cobalt Coordination Polymer with Dicyanamide and 2-Aminopyridine*, Int. J. Inorg. Chem., pp. 9–12, 2015.

[6] Mehta, J. V., Gajera, S. B., Raval, D. B., Thakkar, V. R. & Patel, M. N., *Biological Assessment of Substituted Quinoline Based Heteroleptic Organometallic Compounds*, Medchemcomm, **7**(8), pp. 1617–1627, 2016.

[7] Lipunova, G. N., Nosova, E. V., Charushin, V. N. & Chupakhin, O. N., *Structural, Optical Properties, and Biological Activity of Complexes Based on Derivatives of Quinoline, Quinoxaline, and Quinazoline with Metal Centers from Across the Periodic Table*, Comments Inorg. Chem., **34**(5–6), pp. 142–177, 2014.

[8] Kljun, J. & Turel, I., *Biological Activity of Ruthenium Complexes with Quinoline Antibacterial and Antimalarial Drugs, in Holder*, A. A., Lilge, L., Browne, W. R., Lawrence, M. A. W., and Jr, J. L. B. (Eds.), Ruthenium Complexes: Photochemical and Biomedical Applications, Walter de Gruyter GmbH, London, pp. 239–255, 2017.

[9] Zou, X. Z., Zhang, J. A., Zhang, L. J., Liu, Y. J., Li, N., Li, Y., Wei, S. C. & Pan, M., *Crystal Structures and Biological Activities of a Symmetrical Quinoline Thioether Ligand and Its Transition Metal Complexes*, Inorg. Chem. Commun., **54**, pp. 21–24, 2015.

[10] Sani, U. & Iliyasu, S. M., *Synthesis, Characterization and Antimicrobial Studies on Schiff Base Derived from 2-Aminopyridine and 2-Methoxybenzaldehyde and Its Cobalt(II) and Nickel(II) Complexes*, Bayero J. Pure Appl. Sci., **11**(1), pp. 214, 2019.

[11] Ejidike, I. P. & Ajibade, P. A., *Transition Metal Complexes of Symmetrical and Asymmetrical Schiff Bases as Antibacterial, Antifungal, Antioxidant, and Anticancer Agents: Progress and Prospects*, Rev. Inorg. Chem., **35**(4), pp. 191–224, 2015.

[12] Al-Shaalan, N. H., *Synthesis, Characterization and Biological Activities of Cu(II), Co(II), Mn(II), Fe(II), and UO_2(VI) Complexes with A New Schiff Base hydrazone: O-hydroxyacetophenone-7-chloro-4-quinoline hydrazone*, Molecules, **16**(10), pp. 8629–8645, 2011.

[13] Kurtar, S. N. K., Koçer, F. & Kose, M., *Monomeric and 1D Polymeric Cu(II) Complexes Derived from Dicyanamide: Structural, Characterization, and Antibacterial Properties*, J. Struct. Chem., **61**(8), 1296–1305, 2020.

[14] Tabrizi, L., Chiniforoshan, H. & McArdle, P., *A Novel One-Dimensional Manganese(II) Coordination Polymer Containing Both Dicyanamide and Pyrazinamide Ligands: Synthesis, Spectroscopic Investigations, X-Ray Studies, and Evaluation of Biological Activities*, Spectrochim. Acta - Part A Mol. Biomol. Spectrosc., **139**, pp. 307–312, 2015.

[15] Zheng, L.-L., *Synthesis, Crystal Structures, and Magnetic Properties of Ternary M(II)-Dicyanamide-hydroxypyridine Complexes*, J. Inorg. Chem., **2013**(II), pp. 1–10, 2013.

[16] Mautner, F. A., Jantscher, P., Fischer, R. C., Torvisco, A., Vicente, R., Karsili, T. N. V. & Massoud, S. S., *Synthesis and Characterization of 1D Coordination Polymers of Metal(II)-dicyanamido Complexes*, Polyhedron, **166**, 36–43, 2019.

[17] Mautner, F. A., Jantscher, P. V., Fischer, R. C., Torvisco, A., Reichmann, K., Salem, N. M. H., Gordon, K. J., Louka, F. R. & Massoud, S. S., *Coordination Polymers in Dicyanamido-Cadmium(II) with Diverse Network Dimensionalities*, Crystals, **11**(2), pp. 1–13, 2021.

[18] Mirzaei, M., Eshtiagh-Hosseini, H., Bolouri, Z., Rahmati, Z., Esmaeilzadeh, A., Hassanpoor, A., Bauza, A., Ballester, P., Barceló-Oliver, M., Mague, J. T., Notash, B. & Frontera, A., *Rationalization of Noncovalent Interactions Within Six New MII/8-Aminoquinoline Supramolecular Complexes*, Cryst. Growth Des., **15**(3), pp. 1351–1361, 2015.

[19] Dasna, I. W., Golhen, S., Ouahab, L. & Subakti, *Synthesis, Single Crystal Structure, and Magnetic Properties of 3-D* $Cu(NITpPy)_2[Cu(CN)_3].2CH_3OH.2H_2O$ *Complexes*, IOP Conf. Ser. Mater. Sci. Eng., **202**(1), 2017.

[20] Kundu, S., Roy, S., Bhar, K., Ghosh, R., Lin, C. H., Ribas, J. & Ghosh, B. K., *Syntheses, Structures and Magnetic Properties of Two One-Dimensional Coordination Polymers of Cobalt(II) and Nickel(II) Dicyanamide Containing a Tridentate N-donor Schiff Base*, J. Mol. Struct., 1038, 78–85, 2013.

[21] Eberle, B., Herrmann, H., Kaifer, E. & Himmel, H. J., *Redox Reactions Between Guanidine Electron Donors and Silver Dicyanamide: Synthesis of C, N Material Precursors and Coordination Polymers*, Eur. J. Inorg. Chem., **2**(21), pp. 3671–3679, 2013.

[22] Mehta, K. V., *Synthesis, Characterization, and Antimicrobial Activity of Some Heterocyclic Compounds and Its Metal Complexes*, Silpakorn U Sci. Tech J., **2**(8), pp. 62–70, 2014.

[23] Anacona, J. R., Ruiz, K., Loroño, M. & Celis, F., *Antibacterial Activity of Transition Metal Complexes Containing a Tridentate NNO Phenoxymethylpenicillin-Based Schiff Base. An Anti-MRSA Iron(II) Complex*, Appl. Organomet. Chem., **33**(4), pp. 1–9, 2019.

[24] Dasna, I., Golhen, S., Ouahab, L., Peña, O., Daro, N. & Sutter, J. P., *Ferromagnetic Interactions in 0D and 2D Mn(II) Coordination Complexes Containing Nitronyl-Nitroxide Radicals and Dicyanamide Anions: CH3CN*, Comptes Rendus l'Academie des Sci. - Ser. IIC Chem., **4**(2), pp. 125–133, 2001.

[25] Dasna, I., Golhen, S., Ouahab, L., Daro, N. & Sutter, J. P., *Synthesis, X-Ray Crystal Structures and Magnetic Properties of* Cu^{ii} *and* Mn^{ii} *Complexes Containing Imino Nitroxide Radicals and A Dicyanamide Anion*, New J. Chem., **25**(12), pp. 1572–1576, 2001.

[26] Chakraborty, P. & Dasgupta, S., *Synthesis of One-Dimensional Coordination Polymer using Dicyanamide Spacer to Explore Catecholase Like Activity*, Polyhedron, **188**, 114700, 2020.

[27] Setifi, Z., Geiger, D., Jelsch, C., Maris, T., Glidewell, C., Mirzaei, M., Arefian, M., Setifi, F., *The First Fe(II) Complex Bearing end-to-end Dicyanamide as a Double Bridging Ligand: Crystallography Study and Hirshfeld Surface Analysis; Completed with a CSD Survey*, Journal of Molecular Structure, **1173**(II), pp. 697-706, 2018.

[28] Lopes, L. B. Corrêa, C. C., Guedes, G. P., Vaz, M. G. F., Diniz, R., Machado, F. C., *Two New Coordination Polymers Involving Mn(II), Co(II), Dicyanamide Anion and The Nitrogen Ligand 5,5'-Dimethyl-2,2'-Dipyridine: Crystal Structures and Magnetic Properties*, Polyhedron, **50**(1), pp. 16–21, 2013.

[29] Mbani, A. L. O., Yufanyi, D. M., Tabong, C. D., Hubert, N. J., Yuoh, A. C. B., Paboudam, A. G. & Ondoh, A.M., *Synthesis, Crystal Structure, DFT Studies and Hirshfeld Surface analysis of Manganese(II) and Cadmium(II) Coordination Polymers of 2-aminopyridine and Dicyanamide*, J. Mol. Struct., **1261**, 132956, 2022.

[30] Hindi, K. M., Panzner, M. J., Tessier, C. A., Cannon, C. L. & Youngs, W. J., 2009, *The Medicinal Applications of Imidazolium Carbene-metal Complexes*, Chem. Rev., **109**(8), pp. 3859–3884, 2009.